Intraseasonal Predictions for the South American Rainfall Dipole

Nicolás Díaz[1], Marcelo Barreiro[1], and Nicolás Rubido[1,2,3]

[1]Universidad de la República, Instituto de Física de Facultad de Ciencias, Iguá 4225, Montevideo, Uruguay.
[2]University of Aberdeen, Aberdeen Biomedical Imaging Centre, AB25 2ZG Aberdeen, United Kingdom.
[3]University of Aberdeen, Institute for Complex Systems and Mathematical Biology, AB24 3UE Aberdeen, United Kingdom.

Key Points:

- Introduce a method to find statistically significant transitions between the quantile states of stationary time-series.
- Reveal forecasting windows at intraseasonal time-scales for tercile and quartile states of the South American rainfall Dipole index.
- Report 2 robust and reliable time-windows at 5 to 15 and 60 to 70 days, where we can forecast SAD states with 99% confidence.

Corresponding author: Nicolás Díaz, nicolasdiaznegrin@gmail.com

Abstract

The South American rainfall Dipole (SAD) is a renowned spatial structure present in the austral summer as part of the South American monsoon system. SAD phases have been related with extreme precipitations and severe droughts across South America, but are yet to be predicted. Here, we reveal 2 robust and reliable intraseasonal windows in the accumulated SAD index where we can forecast its quantile-state between 5 to 15 and 60 to 70 days in advance (99% significance level). These windows are insensitive to variations in the pole's size and accumulation window, and results are consistent across different quantiles states (median, tercile, and quartile). Our method, which is based on analysing the lagged mutual information between future and present states, could be used in the development of early-warnings for extreme rainfall events. Moreover, it is unrestricted to the present analysis, being applicable to other stationary signals where a forecast is missing.

Plain Language Summary

The South American Dipole (SAD) is a spatially-extended rainfall system present in the austral summer. Its dipole behaviour means that it is composed of two regions (or poles): when one regions shows an increase in precipitation the other region shows a decrease in precipitation, and vice-versa. Forecasting future SAD behaviour is particularly important as its extreme states have been associated with floods or droughts over these regions (which include highly populated areas, such as São Paulo, Brazil). Here, we introduce a method to predict the dipole's future-state from statistical and information theory analyses. Our main results show that there are two time-windows where forecasting future SAD states is possible: from 5 to 15 days and from 60 to 70 days. These windows belong to the intraseasonal time-scale (from 10 to 90 days), which is a generally challenging time-scale to have predictions and where forecasts are scarce.

1 Introduction

South America (SA) has a broad range of climate behaviours (Garreaud & Aceituno, 2007; Cavalcanti, 2016), both in space and time. This stems from its latitude extension that covers from equatorial to mid latitudes, its topography and heterogeneous vegetation, as well as its dependence on multiple modes of climate variability. Among the latter phenomena, we can highlight SA's climate dependence on El Niño Southern Oscillation (ENSO) at inter-annual time-scales (Ropelewski & Halpert, 1987; Barreiro & Tippmann, 2008; Barreiro, 2010) and the Madden-Julian Oscillation (MJO) at intraseasonal (IS) time-scales (Alvarez et al., 2016, 2017; Shimizu et al., 2017). These are the leading modes on their corresponding time scales and alter regional climate through, for example, modulating the frequency of occurrence of frontal systems, extra-tropical cyclones, or mesoscale convective systems.

Recently, it has been shown that different modes characterize IS variability depending on the season (C. S. Vera et al., 2018). The wet season (October-April) is characterized by the presence of a dipole-like spatial structure, which can be revealed by a principal component analysis of the rainfall field. This structure is known as the South American rainfall Dipole (SAD) (Nogués-Paegle & Mo, 1997; Boers et al., 2014), with centers located at the South Atlantic Convergence Zone (SACZ) and over Southeastern South America (SESA). The dry season (May-September), on the other hand, exhibits a monopole behaviour, centered at SESA. In our work we will focus on the SAD during the summer season as it is the rainy season over most of South America.

The SAD characterizes the IS variability of the South American Monsoon System (SAMS) (C. Vera et al., 2006; Barros et al., 2002), and has been mainly related to the activity of the MJO (Alvarez et al., 2016, 2017; C. S. Vera et al., 2018). The MJO has

a characteristic time scale of about 30−80 days and can impact South America through two mechanisms: (a) a tropical-tropical one, involving changes in the divergent circulation as the MJO propagates eastward, and (b) a tropical-extratropical one, taking place through the excitation and dispersion of Rossby waves from the Indo-Pacific to the Atlantic region (Paegle et al., 2000; Carvalho et al., 2004; De Souza & Ambrizzi, 2006; Gonzalez & Vera, 2014; Shimizu & Ambrizzi, 2016; Alvarez et al., 2016; Barreiro et al., 2019). In particular, the dipole phase when the SACZ center is enhanced [weakened] and the SESA center is weakened [enhanced], has been associated with phases 8-1 [3-4] of the MJO. Moreover, SAD phases have been related with extreme precipitation events and severe droughts across SA (Carvalho et al., 2002; Boers et al., 2013), which have severe socioeconomic impact in highly populated areas, such as São Paulo or Buenos Aires, and are yet to be predicted. Hence, being able to predict SAD's behaviour at the IS time-scales in order to develop early-warnings for extreme rainfall events is highly important.

In this work, we reveal the existence of intraseasonal (IS) predictability windows in the Accumulated SAD (ASAD) index during the months of December to March. Our methodology is based on defining a quantile-state time-series from the ASAD index and on using the lagged mutual information (MI) to quantify the average amount of information shared by present and future quantile-states. Our results show that, from present quantile-states, we can forecast at 5 to 15 days and 60 to 70 days ahead – to the best of our knowledge, IS forecast at 60 to 70 days has never been achieved before. These two predictability windows emerge robustly, i.e., insensitive to changes in our control parameters (accumulated window size and poles' size), and reliably, i.e., statistically significant at a 99% significance level and consistent across quantile choices (either median, terciles, or quartiles). We also reveal a third robust IS window at approximately 45 days, which only emerges when using quartile-states. In summary, we develop the first IS forecast for the ASAD index based on an approach that can be also applied to find predictions of other stationary time-series.

The paper is organized as follows: Sect. 2 describes the data and our methodology, Sect. 3 shows the main results and analysis, and Sect. 4 has the conclusions.

2 Methods and Data

2.1 Data Specifics and the construction of the SAD index

We consider precipitation data from the Tropical Rainfall Measuring Mission (TRMM). These data consist of a multi-satellite observation net, created to study the rainfall field over the tropics and subtropics. Although the mission (launched in 1997) ended in 2015, the data production was continued through the TRMM Multi-satellite Precipitation Analysis (TMPA) (Huffman et al., 2007). Here, we use daily precipitation from the TMPA 3B42v7, which runs from 1998-01-01 to 2019-12-31 over a $0.25° \times 0.25°$ spatial grid. We only consider the months that the SAMS is in its mature stage (C. Vera et al., 2006), namely, December-January-February-March (DJFM). Thus, we avoid dealing with the developing [vanishing] stages of the transition from dry to wet [wet to dry] months, which introduce biases in the analysis.

In order to define the poles of the South American Dipole (SAD) from the precipitation anomaly fields, we follow the locations found by C. S. Vera et al. (2018). We construct a time-series for each pole by averaging the anomalies within rectangular boxes placed at these 2 locations. Once both space-averaged time-series are defined, we subtract the daily climatology for each time stamp and standardize using the daily standard deviation, resulting in a standardized anomaly time-series for each pole. We then define the SAD index by subtracting the southern pole anomaly to the northern one. We use 3 box-sizes (left panel in Fig. 1) to carry an analysis on the sensitivity of our results to the spatial size of the poles.

In order to filter variability of the SAD on short time-scales, whilst maintaining the intraseasonal (IS) time-scales, we construct an Accumulated SAD (ASAD) index. We do this by adding the SAD daily data within sliding windows of 5, 7, or 9 days (making 1 day sliding-translations of these windows), where we denote the resultant ASAD indexes as $accum5$, $accum7$, or $accum9$, respectively. This smoothing leaves the underlying physics unchanged at the IS time-scale, as we show by testing our results' sensitivity to these 3 time-scales.

2.2 Definition of quantile states and their IS forecasting

The ASAD indexes ($accum5$, $accum7$, or $accum9$) are still too complex and insufficiently long (approximately 2500 data points in 21 years) to make reliable predictions with sufficient statistics. Hence, we transform the ASAD index into a quantized time-series, where each daily data corresponds to the ASAD's quantile-state at the time. We define a 2-state time-series from the distribution's median, 3 states from its terciles, and 4 states from its quartiles. For example, Fig. 1 shows the mean precipitation anomaly fields for the region of interest corresponding to the quartile case. By doing this transformation, we can find statistically significant transition-probabilities between the quantile-states; namely, we can make reliable forecasts. Also, we consider an IS forecast to be robust, only if it is insensitive to the choice of pole size (i.e., size of the boxes on the left panel of Fig. 1) and sliding-window size that defines the ASAD index.

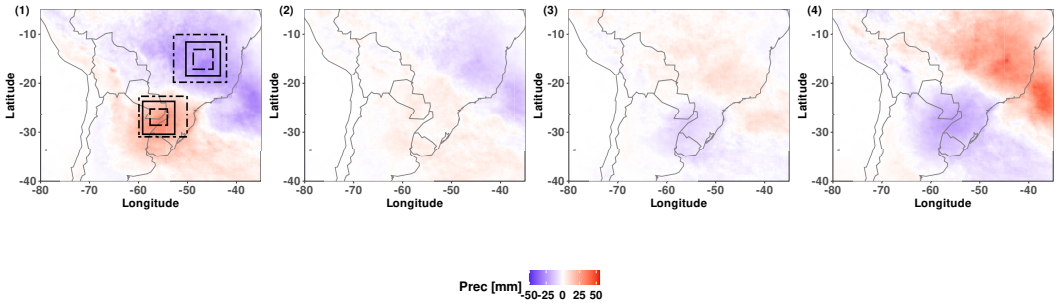

Figure 1. South-American rainfall Dipole (SAD). Panel (1) shows the boxes used to construct the SAD index. From left to right, each panel shows the mean precipitation anomaly field of the accumulated SAD index (using 7 days accumulation windows) for the quartile-states defined over the dotdashed-line box. States (1) and (4) [(2) and (3)] are extreme [neutral] SAD states.

The transition probability of going from state x_i at time t to state x_j at time $t+\tau$ (τ being the time-lag in days), with $i, j = 1, \ldots, N_Q$ (N_Q being the number of quantiles states, e.g., $N_Q = 4$ for quartiles), is

$$P\left(X_{t+\tau} = x_j | X_t = x_i\right) = P_{t,t+\tau}(j|i) \simeq P_\tau(j|i) \simeq \frac{N_\tau(j|i)}{\sum_{j=1}^{N_Q} N_\tau(j|i)}, \tag{1}$$

where X is the states' time-series for one ASAD index, namely, either $accum5$, $accum7$, or $accum9$. The first approximate equality ($P_{t,t+\tau} \simeq P_\tau$) is the assumption of an stationary X, implying that $P_{t,t+\tau}$ is invariant under time-translations and independent of the starting time, t, for all i, j. We achieve this by choosing DJFM months, when the dipole is fully developed. Moreover, our daily standardization removes possible IS cycles that can break time-translation invariance and our time-series length (21 years) is insufficient to include climate-change trends. The last approximate equality is the frequentist approach, where the transition probabilities are the frequency of appearance of

state x_j at time $t+\tau$ when at time t the state was x_i, for all times t and fixed τ, i.e., $N_\tau(j|i)$. We restrict $N_\tau(j|i)$ to consider only causal transitions, namely, transitions between states from the same DJFM period. Overall, $P_\tau(j|i)$ is our forecast.

In order to reliably select only the statistically significant forecasts, we construct a proportion test for Eq. (1). The null-hypothesis (NH) for it is that $X_t = x_i$ and $X_{t+\tau} = x_j$ are statistically independent, which implies that $P_\tau(j|i) = P(j)$ (i.e., the conditional probability is independent of the starting state and equal to the marginal probability of the ending state, $P(j)$). This NH is a Bernoulli process with 2 states: either $P(j)$ or $1-P(j)$. We discard the NH at the 99% significance level only when $P_\tau(j|i)$ falls outside the z_{ij}-score's 99% central values. Specifically, the z_{ij}-score for each $P_\tau(j|i) = P(j)$ is

$$z_{ij} = \frac{P\left(X_{t+\tau} = x_j | X_t = x_i\right) - P\left(X = x_j\right)}{\sqrt{P\left(X = x_j\right)\left[1 - P\left(X = x_j\right)\right]/T}}, \tag{2}$$

where $P\left(X = x_j\right)$ is the marginal probability for the state x_j, with $i, j = 1, \ldots, N_Q$, and the denominator is the standard deviation for this Bernoulli process with T realisations. Given that z_{ij} distributions are asymptotically Gaussian, our 99% significance level is the Gaussian $z \approx 2.576$, which is our boundary to consider $P_\tau(j|i) \neq P(j)$.

3 Results and Analysis

3.1 Instraseasonal predictability windows

We begin by comparing the time-series, *accum*, that result from using different pole sizes (see the 3 boxes in Fig. 1), which we define to capture the South-American Dipole (SAD) variability at different spatial scales. We quantify their similarities by the Pearson correlation coefficient (and the Spearman correlation; not shown), using a t-test at a 99% significance level. This analysis holds significant correlation values (i.e., p-values < 0.01) for all *accum* indexes, ranging from 0.95 to 0.99 – meaning that all pole sizes have similar time-series. Hence, the SAD's behaviour is captured robustly with either box. In what follows, we focus on the results from the largest (pole) box.

Without loss of generality, we show results for tercile and quartile states of the Accumulated SAD (ASAD) indexes. In particular, tercile statistics are commonly used in operational seasonal forecasting – defining positive, neutral, and negative dipole states. Quartile statistic's allow us to differentiate between extreme events – defining 2 extreme positive and negative states and 2 intermediate states – as well as to compare its results with the median case (see Supporting Information). Also, these quantile choices allows to have enough data for all transition probabilities, $P_\tau(j|i)$ [Eq. (1)].

In Fig. 2 we show $P_\tau(j|i)$ for the quartile states ($N_Q = 4$ in Eq. 1) of the ASAD indexes: *accum*5, *accum*7, and *accum*9. Marginal probabilities, $P(j)$, are signalled in all panels (as reference) by an horizontal, black, dashed line (which happens when the starting state does not influence the ending state). Panels are arranged from top to bottom (rows) according to the starting quartile-state, x_i, at time t, and from left to right (columns) according to the ending quartile-state, x_j, at time $t+\tau$. The significant [insignificant] $P_\tau(j|i)$ values are shown with solid [transparent] symbols. We can distinguish the IS windows where a reliable forecast is possible, as the times τ where all 3 indexes have significant $P_\tau(j|i)$ values. Within these windows, we can forecast SAD quartile-states transitions robustly and reliably; namely, the $P_\tau(j|i)$ values that are insensitive to parameter variations and are consistent across spatial and temporal scales.

Our main interest is to find intra-seasonal (IS) predictability-windows that are robust and reliable, disregarding the particular quartile-state (or tercile-state) transition that could be happening. In other words, we want to know when we can forecast the SAD states for any accumulated window-size or quantile-state. We do these by using the lagged Mutual Information (MI), $I(X_t; X_{t+\tau})$, which measures the average shared information

between the states at time t and $t+\tau$, and is defined by (Cover & Thomas, 2012)

$$I(X_t; X_{t+\tau}) = \sum_{i=1}^{N_Q} \sum_{j=1}^{N_Q} P\left(X_t = x_i, X_{t+\tau} = x_j\right) \log_2 \left[\frac{P\left(X_t = x_i, X_{t+\tau} = x_j\right)}{P\left(X_t = x_i\right) P\left(X_{t+\tau} = x_j\right)} \right], \quad (3)$$

$P\left(X_t = x_i, X_{t+\tau} = x_j\right) = P\left(X_t = x_i\right) P\left(X_{t+\tau} = x_j | X_t = x_i\right)$ being the joint probability of having state x_i at time t and state x_j at time $t+\tau$. We note that $I(X_t; X_{t+\tau}) = 0$ when $P\left(X_t = x_i, X_{t+\tau} = x_j\right) = P\left(X_t = x_i\right) P\left(X_{t+\tau} = x_j\right)$ for all i, j, corresponding to independent starting and ending states.

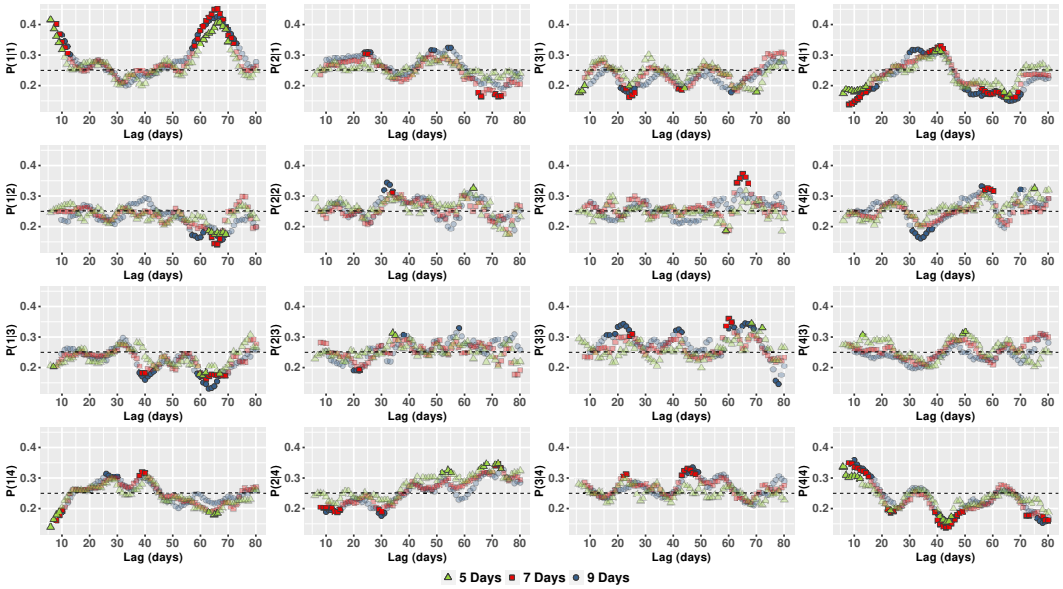

Figure 2. Transition probabilities, $P(j|i)$, between quartile-states of the Accumulated South-American rainfall Dipole (ASAD) index. $P(j|i)$ is shown as a function of the time difference, τ, between the starting quartile state i and the ending quartile state j ($i, j = 1, \ldots, 4$). Panels are organised in rows and columns according to the initial and final quartile-state, respectively. Window sizes of 5, 7, and 9 days used to construct the ASAD indexes, are shown by green triangles, red squares, and blue circles, respectively. Statistical dependence of state j to state i (at the 99% significance level) are signalled by solid symbols and statistical independence (i.e., null hypothesis) by transparent symbols.

Figure 3 shows $I(X_t; X_{t+\tau})$ for all *accum* indexes, following the symbols and colours in Fig. 2. Left [right] panel shows the resultant MI for the quartile [tercile] states. Confidence Intervals (CIs) at the 99% significance level are shown as transparent shaded areas for each *accum* index, which correspond to variables X_t and $X_{t+\tau}$ being statistically independent. These CIs are constructed by randomly resampling (with replacement) 10^3 times the original time-series, where the objective is to construct a surrogate X_t and a $X_{t+\tau}$ time-series. Also, for each *accum* index, the MI starts at different time lags, τ, because we discard the τ lags belonging to the accumulation window (namely, 5, 7, and 9 days), which naturally share information by construction.

From both panels in Fig. 3, we can highlight 2 robust intra-seasonal (IS) predictability windows where ASAD transitions can be predicted with 99% confidence (namely, values outside the shaded areas in either panel). Specifically, these windows – sharing significant information between the present and future ASAD states – are found at $\tau \approx$

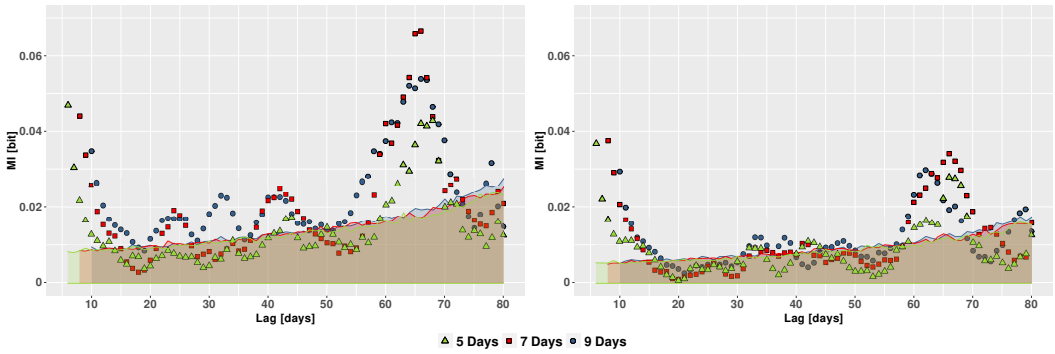

Figure 3. Lagged Mutual Information (MI) between quantile states of the accumulated precipitation anomalies of South American Dipole. Left [Right] panel shows the MI for the quartile-states [tercile-states] as a function of the time lag, τ, between starting and ending state. The symbols and colours are the same as in Fig. 2. Shaded areas at the bottom correspond to the MI values of statistically independent surrogates at a 99% significance level.

5 to 15 days and at $\tau \approx 60$ to 70 days. We note that these windows also appear in our median analysis (see Supporting Information), making them a reliable forecast and possibly arising due to persistence and due to the impact of the MJO, respectively. We also note other predictability-windows on the left panel of Fig. 3, at IS scales of $\tau \approx 25$, $\approx$ 35, and ≈ 45 days. However, these windows are sensitive to the accumulated window-size – with the exception of the quartile-state MI at $\tau \approx 45$ days. In particular, MI values for the *accum*5 index at $\tau \approx 25$ and ≈ 35 fall within the shaded areas, and all *accum* indexes fall within shaded areas for the terciles; as can be seen on the right panel of Fig. 3. Hence, we deem these other predictability-windows as unreliable indicators for IS forecasting. In spite of this inconsistency in the forecasts, we obtain robust results for the quartile-states at $\tau \approx 45$ days (namely, all ASAD indexes show a significant MI value for this window), which could also be related to the MJO.

3.2 Forecasting states of the South-American rainfall dipole

Having identified robust and reliable intraseasonal (IS) predictability-windows from Fig. 3, we can now critically analyse the state-transitions in Fig. 2, which are the reason for having these predictability windows. This analysis is particularly relevant when the final quartile-state for which we can get information from the present is an extreme ASAD state. Physically, the smallest [largest] quartile corresponds to the southern [northern] pole having larger anomalies than the northern [southern] pole for about 5, 7 or 9 days (depending on the *accum* index). More importantly, from a practical point-of-view, identifying the relevant predictability-windows allows to have concise forecasts for particular ASAD states. For example, by fixing τ (horizontal coordinate) and the starting quartile-state (row panels) in Fig. 2, we can directly state the probability of transitioning to any of the 4 possible quartiles in τ days.

The first robust and reliable IS predictability window in Fig. 3 happens at $\tau \approx 5$ to 15 days. As can be seen from the top- and bottom-corner panels in Fig. 2, this window has significant MI values because of transitions happening between extreme quartile-states, i.e., states 1 and 4 (or tercile-states; see, for example, Fig. S1 in Supporting Information). Particularly, the top [bottom] left and bottom [top] right panels show $P(1|1)$ $[P(1|4)]$ and $P(4|4)$ $[P(4|1)]$ having significantly higher [lower] probabilities than the marginal case, i.e., $P(1) = P(4) = 1/4$, respectively. On the other hand, the remaining neutral states, i.e., quartiles 2 and 3, show unconditional transitions to and from them, with all

transition probabilities similar to the corresponding marginal probabilities (e.g., $P(2|2) \simeq P(2)$, $P(2|3) \simeq P(3)$, or $P(3|4) \simeq P(4)$). Hence, this predictability-window has the following characteristics: likely persistence of extreme quartile-states ($P(1|1)$ or $P(4|4) > 30\%$), unlikely transitioning between opposite extreme quartile-states ($P(4|1)$ or $P(1|4) < 20\%$), and independent neutral quartile-states ($P(i|j) \simeq P(j)$).

This persistent behaviour in the transitions to and from extreme ASAD quartile-state can be understood by considering them as the opposite phases for the SAD. This means that it would be expected to be persistent whilst the SAD is in a particular phase for this time-scale – to the best of our knowledge, our statistical analysis is the first to report on the events duration. Also, we highlight that the time-scale of this predictability-window is larger than the persistence time-scale that one would expect for synoptic phenomena, which is a significant improvement in the forecasting of SAD index's future-states.

The second robust and reliable IS predictability window in Fig. 3 happens at $\tau \approx$ 60 to 70 days. As can be seen from the left column panels in Fig. 2, this window has significant MI values, mainly, because of transitions happening to the first quartile-state, $P(1|j)$. Another contribution to this window's predictability comes from a decrease in the probability of transitioning from the extreme state 1 to the extreme state 4, i.e., $P(4|1) < 20\%$ (top right panel in Fig. 2). Secondary contributions appear inconsistently across other quartile states, such as $P(1|3)$ and $P(3|3)$, where transition probabilities are significant only for specific window-size accumulations. Overall, we believe that this IS time-window is a consequence of the Madden-Julian Oscillation (MJO), which has characteristic time-scales ranging from 30 to 80 days and influences the occurrence of SAD phases.

As a working example, we can consider a forecast for $\tau = 10$ days. When the present ASAD index has a value in quartile 1 [4], $P(1|1) \simeq 0.33$ and $P(4|1) \simeq 0.18$ [$P(4|4) \simeq 0.33$ and $P(1|4) \simeq 0.18$] after 10 days, where the remaining transitions in Fig. 2 from and to states 2 and 3 show inconclusive results. Similarly, we can make a forecast for $\tau =$ 45 days. This particular forecast is only possible for quartile states, but it shows some insensitivity to the accumulation window and box size. For example, when the present ASAD index has a value in quartile 1 [4], $P(4|1) \simeq 0.33$ [$P(1|4) \simeq 0.18$] after 45 days. Overall, our methodology allows for the construction of transition probabilities, such as those in Fig. 2, which allow to develop intraseasonal forecasts for the SAD states.

4 Conclusions

We employed a methodology based on statistical and information theory analysis, with the objective of studying intraseasonal (IS) predictability over the South-American rainfall Dipole (SAD). By working with DJFM months, we are certain that the dipole system is in its mature stage and the time series have an stationary behaviour. We defined the ASAD index – for 1 day sliding windows of accumulated rainfall anomalies of 5, 7 and 9 days – and introduced a finite set of states based on its quantiles (i.e., median, terciles and quartiles). By doing this, we reduced the complexity of the ASAD index and were able to study the possible transitions between initial and final states (lagged by a time τ) with sufficient statistics.

By computing the lagged mutual information, we found that there are two IS time windows where the initial and final states share significant information (at a 99% significance level). Both of them were found robustly and reliably by taking into account the SAD index space-variability (i.e., poles' sizes), the accumulation window for the ASAD-index construction, and the quantile-states considered.

The first time window is found from $\tau \approx 5$ to 15 days. We interpret this window as a persistence-like behaviour, which extends beyond the synoptic time-scale. The predictable states in this time window are the extreme ones (both for terciles and quartiles), which can be associated with the dipole phases. Hence, the persistence behaviour could

be interpreted as a mean-time duration of the dipole phases. The second time window goes from $\tau \approx 60$ to 70 days. This result is consistent with the impact of the Madden-Julian Oscillation (MJO) on the intraseasonal time-scales variability of the SAD.

Finally, we remark that by critically analyzing the specific transitions involved in each time window, we can forecast future states of the SAD by operationally observing the present states of the system for about 5 to 9 days. This allows, for the first time, to develop a quantile-based operational forecast system at IS time-scales of the extreme phases of the main mode of rainfall variability in South America.

Acknowledgments

All authors acknowledge PEDECIBA, Uruguay. N.D. acknowledges Comisión Académica de Posgrado (CAP), Uruguay. N.R. acknowledges the Comisión Sectorial de Investigación Científica (CSIC), Uruguay, group grant "CSIC2018 - FID13 - grupo ID 722". The data used is in this work is available from TRMM (TMPA) products at `10.5067/TRMM/TMPA/DAY/7`.

References

Alvarez, M. S., Vera, C. S., & Kiladis, G. N. (2017). Mjo modulating the activity of the leading mode of intraseasonal variability in south america. *Atmosphere*, *8*(12), 232.

Alvarez, M. S., Vera, C. S., Kiladis, G. N., & Liebmann, B. (2016). Influence of the madden julian oscillation on precipitation and surface air temperature in south america. *Climate Dynamics*, *46*(1-2), 245–262.

Barreiro, M. (2010). Influence of enso and the south atlantic ocean on climate predictability over southeastern south america. *Climate dynamics*, *35*(7-8), 1493–1508.

Barreiro, M., Sitz, L., de Mello, S., Franco, R. F., Renom, M., & Farneti, R. (2019). Modelling the role of atlantic air–sea interaction in the impact of madden–julian oscillation on south american climate. *International Journal of Climatology*, *39*(2), 1104–1116.

Barreiro, M., & Tippmann, A. (2008). Atlantic modulation of el nino influence on summertime rainfall over southeastern south america. *Geophysical Research Letters*, *35*(16).

Barros, V., Doyle, M., González, M., Camilloni, I., Bejarán, R., & Caffera, R. M. (2002). Climate variability over subtropical south america and the south american monsoon: a review. *Meteorologica*, *27*(1), 33–57.

Boers, N., Bookhagen, B., Marwan, N., Kurths, J., & Marengo, J. (2013). Complex networks identify spatial patterns of extreme rainfall events of the south american monsoon system. *Geophysical Research Letters*, *40*(16), 4386–4392.

Boers, N., Rheinwalt, A., Bookhagen, B., Barbosa, H. M., Marwan, N., Marengo, J., & Kurths, J. (2014). The south american rainfall dipole: a complex network analysis of extreme events. *Geophysical Research Letters*, *41*(20), 7397–7405.

Carvalho, L. M., Jones, C., & Liebmann, B. (2002). Extreme precipitation events in southeastern south america and large-scale convective patterns in the south atlantic convergence zone. *Journal of Climate*, *15*(17), 2377–2394.

Carvalho, L. M., Jones, C., & Liebmann, B. (2004). The south atlantic convergence zone: Intensity, form, persistence, and relationships with intraseasonal to interannual activity and extreme rainfall. *Journal of Climate*, *17*(1), 88–108.

Cavalcanti, I. F. (2016). *Tempo e clima no brasil*. Oficina de textos.

Cover, T. M., & Thomas, J. A. (2012). *Elements of information theory*. John Wiley & Sons.

De Souza, E. B., & Ambrizzi, T. (2006). Modulation of the intraseasonal rainfall over tropical brazil by the madden–julian oscillation. *International Journal*

of Climatology: A Journal of the Royal Meteorological Society, *26*(13), 1759–1776.

Garreaud, R. D., & Aceituno, P. (2007). Atmospheric circulation over south america: mean features and variability. *The physical geography of South America. Oxford University Press, Oxford, England*.

Gonzalez, P. L., & Vera, C. S. (2014). Summer precipitation variability over south america on long and short intraseasonal timescales. *Climate dynamics*, *43*(7-8), 1993–2007.

Huffman, G., Adler, R., Bolvin, D., Gu, G., Nelkin, E., Bowman, K., ... Wolff, D. (2007, 02). The trmm multisatellite precipitation analysis (tmpa): Quasi-global, multiyear, combined-sensor precipitation estimates at fine scales. *Journal of Hydrometeorology - J HYDROMETEOROL*, *8*. doi: 10.1175/JHM560.1

Nogués-Paegle, J., & Mo, K. C. (1997). Alternating wet and dry conditions over south america during summer. *Monthly Weather Review*, *125*(2), 279–291.

Paegle, J. N., Byerle, L. A., & Mo, K. C. (2000). Intraseasonal modulation of south american summer precipitation. *Monthly Weather Review*, *128*(3), 837–850.

Ropelewski, C. F., & Halpert, M. S. (1987). Global and regional scale precipitation patterns associated with the el niño/southern oscillation. *Monthly weather review*, *115*(8), 1606–1626.

Shimizu, M. H., & Ambrizzi, T. (2016). Mjo influence on enso effects in precipitation and temperature over south america. *Theoretical and applied climatology*, *124*(1-2), 291–301.

Shimizu, M. H., Ambrizzi, T., & Liebmann, B. (2017). Extreme precipitation events and their relationship with enso and mjo phases over northern south america. *International Journal of Climatology*, *37*(6), 2977–2989.

Vera, C., Higgins, W., Amador, J., Ambrizzi, T., Garreaud, R., Gochis, D., ... others (2006). Toward a unified view of the american monsoon systems. *Journal of climate*, *19*(20), 4977–5000.

Vera, C. S., Alvarez, M. S., Gonzalez, P. L., Liebmann, B., & Kiladis, G. N. (2018). Seasonal cycle of precipitation variability in south america on intraseasonal timescales. *Climate Dynamics*, *51*(5-6), 1991–2001.